



**Queensland University of Technology**  
Brisbane Australia

This is the author's version of a work that was submitted/accepted for publication in the following source:

Frost, Ray L., Couperthwaite, Sara J., & Xi, Yunfei (2012) Vibrational spectroscopy of the multianion mineral kemmlitzite (Sr,Ce)Al<sub>3</sub>(AsO<sub>4</sub>)(SO<sub>4</sub>)(OH)<sub>6</sub>. *Spectroscopy Letters*, 45(7), pp. 482-486.

This file was downloaded from: <http://eprints.qut.edu.au/57894/>

**© Copyright 2012 Taylor & Francis Group**

This is a preprint of an article submitted for consideration in the *Spectroscopy Letters* © 2012 [copyright Taylor & Francis]; *Spectroscopy Letters* is available online at: [www.tandfonline.com](http://www.tandfonline.com)

**Notice:** *Changes introduced as a result of publishing processes such as copy-editing and formatting may not be reflected in this document. For a definitive version of this work, please refer to the published source:*

<http://dx.doi.org/10.1080/00387010.2011.618519>

1 **Vibrational spectroscopy of the multianion mineral kemmlitzite**



3  
4 **Ray L. Frost, \* Sara J. Palmer and Yunfei Xi**

5  
6 Chemistry Discipline, Faculty of Science and Technology, Queensland University of  
7 Technology, GPO Box 2434, Brisbane Queensland 4001, Australia.  
8

9 **Abstract**

10 Some minerals are colloidal and show no X-ray diffraction patterns. Vibrational  
11 spectroscopy offers one of the few methods for the assessment of the structure of these types  
12 of mineral. Among this group of minerals is kemmlitzite  $(\text{Sr,Ce})\text{Al}_3(\text{AsO}_4)(\text{SO}_4)(\text{OH})_6$ . The  
13 objective of this research is to determine the molecular structure of the mineral kemmlitzite  
14 using vibrational spectroscopy. Raman microscopy offers a useful method for the analysis of  
15 such colloidal minerals.

16 Raman and infrared bands are attributed to the  $\text{AsO}_4^{3-}$ ,  $\text{SO}_4^{2-}$  and water stretching vibrations.  
17 The Raman spectrum is dominated by a very intense sharp band at  $984\text{ cm}^{-1}$  assigned to the  
18  $\text{SO}_4^{2-}$  symmetric stretching mode. Raman bands at  $690$ ,  $772$  and  $825\text{ cm}^{-1}$  may be assigned to  
19 the  $\text{AsO}_4^{3-}$  antisymmetric and symmetric stretching modes. Raman bands observed at  $432$   
20 and  $465\text{ cm}^{-1}$  are attributable to the doubly degenerate  $\nu_2(\text{SO}_4)^{2-}$  bending mode. Vibrational  
21 spectroscopy is important in the assessment of the molecular structure of the kemmlitzite,  
22 especially when the mineral is non-diffracting or poorly diffracting.

23 **Keywords:** Raman spectroscopy, kemmlitzite, beudantite, arsenate, sulphate  
24  
25  
26

---

\* Author to whom correspondence should be addressed (r.frost@qut.edu.au)

27

## 28 **Introduction**

29 Kemmlitzite is a rare secondary mineral found in the zone of oxidized over lead-bearing  
30 deposits. Kemmlitzite  $(\text{Sr,Ce})\text{Al}_3(\text{AsO}_4)(\text{SO}_4)(\text{OH})_6$  [1] is a multi-anion mineral containing  
31 hydroxyl, sulphate and arsenate groups and is a member of the beudantite subgroup of  
32 alunites [2-4]. The mineral is a source of rare earth elements. The mineral is hexagonal with  
33 Point Group  $3\ 2/m$  and Space Group  $[R\bar{3}m]$  [2, 5]. Kemmlitzite was originally described as  
34 hidalgoite. It occurs as trigonal, pseudo cubic, colourless to white crystals of 0.2 to 3 mm.  
35 Kemmlitzite is found together with albite, quartz, cabalzarite, tripuhyite, tilasite and  
36 arseniosiderite. The mineral has the potential to act as a gas sensor.

37

38 The reason for this research is that minerals such as kemmlitzite are found in soils and in old  
39 mine sites. Further, the formation of kemmlitzite can be used as the basis for arsenic  
40 accumulation. Therefore, this research focuses on the spectroscopic determination of  
41 kemmlitzite and consequential molecular structure. Raman spectroscopy has proven very  
42 useful for the study of minerals [6-13]. Indeed Raman spectroscopy has proven most useful  
43 for the study of diagenetically related minerals as often occurs with minerals containing  
44 arsenate and sulphate groups, including pitticite and zykaite. Raman spectroscopy is  
45 especially useful when the minerals are X-ray non-diffracting or poorly diffracting and very  
46 useful for the study of amorphous and colloidal minerals. Kemmlitzite is a mineral which  
47 falls into this category. This paper is a part of systematic studies of vibrational spectra of  
48 minerals of secondary origin in the oxide supergene zone. In this work we attribute bands at  
49 various wavenumbers to vibrational modes of kemmlitzite using Raman spectroscopy and  
50 relate the spectra to the structure of the mineral.

51

## 52 **Experimental**

### 53 **Minerals**

54 The mineral kemmlitzite was supplied by The Mineralogical research Company. The  
55 mineral originated from Kemmlitz Deposit, Oschatz, Sachsen, Germany. Details of the  
56 mineral have been published [14].

## 57 **Raman spectroscopy**

58 Crystals of kemmlitzite were placed on a polished metal surface on the stage of an Olympus  
59 BHSM microscope, which is equipped with 10x, 20x, and 50x objectives. The microscope is  
60 part of a Renishaw 1000 Raman microscope system, which also includes a monochromator, a  
61 filter system and a CCD detector (1024 pixels). The Raman spectra were excited by a  
62 Spectra-Physics model 127 He-Ne laser producing highly polarised light at 633 nm and  
63 collected at a nominal resolution of  $2\text{ cm}^{-1}$  and a precision of  $\pm 1\text{ cm}^{-1}$  in the range between  
64 100 and  $4000\text{ cm}^{-1}$ . Repeated acquisition on the crystals using the highest magnification (50x)  
65 was accumulated to improve the signal to noise ratio in the spectra. Spectra were calibrated  
66 using the  $520.5\text{ cm}^{-1}$  line of a silicon wafer.

## 67 **Infrared spectroscopy**

68 Infrared spectra were obtained using a Nicolet Nexus 870 FTIR spectrometer with a smart  
69 endurance single bounce diamond ATR cell. Spectra over the  $4000\text{--}525\text{ cm}^{-1}$  range were  
70 obtained by the co-addition of 128 scans with a resolution of  $4\text{ cm}^{-1}$  and a mirror velocity of  
71  $0.6329\text{ cm/s}$ . Spectra were co-added to improve the signal to noise ratio.

72 Band component analysis was undertaken using the Jandel 'Peakfit' (Erkrath,  
73 Germany) software package which enabled the type of fitting function to be selected and  
74 allowed specific parameters to be fixed or varied accordingly. Band fitting was done using a  
75 Lorentz-Gauss cross-product function with the minimum number of component bands used  
76 for the fitting process. The Lorentz-Gauss ratio was maintained at values greater than 0.7 and  
77 fitting was undertaken until reproducible results were obtained with squared correlations ( $r^2$ )  
78 greater than 0.995. Band fitting of the spectra is quite reliable providing there is some band  
79 separation or changes in the spectral profile.

## 80 **Results and discussion**

81 The Raman spectrum of kemmlitzite in the  $550\text{ to }1150\text{ cm}^{-1}$  region and of a second  
82 kemmlitzite crystal in the  $500\text{ to }900\text{ cm}^{-1}$  region are displayed in **Figures 1a and 1b**. The  
83 spectra are different and this is attributed to an orientation effect. In **Figure 1a** the intense  
84 peak at  $984\text{ cm}^{-1}$  with a shoulder at  $957\text{ cm}^{-1}$  is assigned to the  $\text{SO}_4^{2-}$   $\nu_1$  symmetric stretching  
85 mode. In **Figure 1b**, the intense peaks are due to the  $\text{AsO}_4^{3-}$  antisymmetric and symmetric  
86 stretching modes. It is probable that the band at  $825\text{ cm}^{-1}$  is attributed to the  $\text{AsO}_4^{3-}$   
87 symmetric stretching vibration. The other two bands are assigned to the antisymmetric

88 stretching vibrations. The infrared spectrum of kemmlitzite in the 500 to 1800 cm<sup>-1</sup> region is  
89 shown in **Figure 2**. The spectrum is dominated by two intense bands at 851 and 962 cm<sup>-1</sup>.  
90 These bands may be attributed to the AsO<sub>4</sub><sup>3-</sup> and SO<sub>4</sub><sup>2-</sup> stretching vibrations. The bands at  
91 574, 595 and 614 cm<sup>-1</sup> are due to the  $\nu_4$  (SO<sub>4</sub>)<sup>2-</sup> bending modes.

92

93 The Raman spectrum of kemmlitzite in the 100 to 600 cm<sup>-1</sup> range is reported in **Figure 3**. The  
94 Raman bands observed at 388 and 427 cm<sup>-1</sup> are attributable to the doubly degenerate  $\nu_2$   
95 (SO<sub>4</sub>)<sup>2-</sup> bending mode. There is also the possibility that the band at 427 cm<sup>-1</sup> is due to the  
96 triply degenerate bending vibration ( $F_2$ ,  $\nu_4$ ). The strong Raman band at 342 cm<sup>-1</sup> is assigned  
97 to the doubly degenerate bending vibration ( $E$ ,  $\nu_2$ ). The Raman spectrum in the 1000 to 1800  
98 cm<sup>-1</sup> region is reported in **Figure 4**. Three bands may be defined at 1356, 1524 and 1591 cm<sup>-1</sup>.  
99 These bands are attributed to OH deformation modes of OH bonded to large cations.

100 The Raman spectrum of kemmlitzite in the 3000 to 3800 cm<sup>-1</sup> region and the infrared  
101 spectrum in the 2700 to 3100 cm<sup>-1</sup> region are displayed in **Figures 5a and 5b**. In the Raman  
102 spectrum, component bands are found at 3047, 3374, 3441 and 3566 cm<sup>-1</sup>. According to the  
103 formula (Sr,Ce)Al<sub>3</sub>(AsO<sub>4</sub>)(SO<sub>4</sub>)(OH)<sub>6</sub> no water is present in the structure, otherwise a water  
104 bending mode at around 1630 cm<sup>-1</sup> would be expected. These bands are attributed to OH  
105 stretching modes. The observation of multiple OH stretching vibrations suggests that the OH  
106 units are not equivalent. The infrared spectrum shows bands at 2851, 2894, 2923 and 2954  
107 cm<sup>-1</sup>.

108 Studies have shown a strong correlation between OH stretching frequencies and both  
109 O··O bond distances and H··O hydrogen bond distances [15-18]. Libowitzky (1999) showed  
110 that a regression function can be employed relating the hydroxyl stretching wavenumbers  
111 with regression coefficients better than 0.96 using infrared spectroscopy [19]. The function is  
112 described as:  $\nu_1 = (3592 - 304) \times 109^{\frac{-d(O-O)}{0.1321}} \text{ cm}^{-1}$ . Thus OH··O hydrogen bond distances may  
113 be calculated using the Libowitzky empirical function. The values for the OH stretching  
114 vibrations from the Raman spectra shown in the figures provide hydrogen bond distances of  
115 2.6604 Å (3047 cm<sup>-1</sup>), 2.7814 Å (3374 cm<sup>-1</sup>), 2.82899 Å (3441 cm<sup>-1</sup>), 3.0623 Å (3566 cm<sup>-1</sup>)  
116 and from the infrared data 2.6253 Å (2881 cm<sup>-1</sup>), 2.6277 Å (2894 cm<sup>-1</sup>), 2.6333 Å (2923 cm<sup>-1</sup>)  
117 2.6396 Å (2954 cm<sup>-1</sup>). The large hydrogen bond distances which are present in kemmlitzite  
118 can also be seen in other mixed anion minerals such as pitticite and zykaite where the  
119 distances ranging between 3.052(5) and 2.683(6) Å. Such hydrogen bond distances are  
120 typical of secondary minerals. A range of hydrogen bond distances are observed from

121 reasonably strong to weak hydrogen bonding. This range of hydrogen bonding contributes to  
122 the stability of the mineral.

123

124 Two types of OH units can be identified in the structure of kemmlitzite. The hydrogen  
125 bond distances previously established above can be used to predict the hydroxyl stretching  
126 wavenumbers. The spectrum of kemmlitzite may be divided into two groups of OH stretching  
127 wavenumbers; namely 3300–3700  $\text{cm}^{-1}$  and 2900–3300  $\text{cm}^{-1}$ . This distinction suggests that  
128 the strength of the hydrogen bonds as measured by the hydrogen bond distances can also be  
129 divided into two groups according to the H-bond distances. An arbitrary cut-off point may be  
130 2.74 Å based upon the wavenumber 3300  $\text{cm}^{-1}$ . Thus the first three bands at 3374, 3441 and  
131 3566  $\text{cm}^{-1}$  may be described as weak hydrogen bonds and the two bands at 3047 and 3269  
132  $\text{cm}^{-1}$  as relatively strong hydrogen bonds. All of the infrared bands are described as due to  
133 strong hydrogen bonding.

### 134 **Conclusions**

135 Kemmlitzite is an example of a mineral which resembles a gel and as such shows poor X-ray  
136 diffraction patterns. The application of vibrational spectroscopy is of importance as it offers  
137 one of the only methods for the assessment of the molecular structure of the mineral.

138

139 The Raman spectrum of kemmlitzite is dominated by a very intense sharp band at 984  $\text{cm}^{-1}$   
140 assigned to the  $\text{SO}_4^{2-}$  symmetric stretching mode. The same vibrational mode is observed in  
141 the infrared spectrum as a sharp band at 962  $\text{cm}^{-1}$ . Raman bands at 690, 772 and 825  $\text{cm}^{-1}$  are  
142 assigned to  $\text{AsO}_4^{3-}$  antisymmetric and symmetric stretching modes. Infrared bands were  
143 observed at 760, 851 and 962  $\text{cm}^{-1}$ .

144 The observation of multiple bands in the  $\nu_4(\text{SO}_4)^{2-}$  spectral region at 574, 595, 604 and 614  
145  $\text{cm}^{-1}$  in the infrared spectrum supports the concept of reduction in symmetry of the sulphate  
146 anion in the structure of kemmlitzite. Raman bands observed at 427 and 482  $\text{cm}^{-1}$  are  
147 attributable to the doubly degenerate  $\nu_2(\text{SO}_4)^{2-}$  bending mode.

148 Vibrational spectroscopy is important in the assessment of the molecular structure of the  
149 kemmlitzite, especially when the mineral is non-diffracting or poorly diffracting.

### 150 **Acknowledgments**

151 The financial and infra-structure support of the Queensland University of Technology,  
152 Chemistry discipline is gratefully acknowledged. The Australian Research Council (ARC) is  
153 thanked for funding the instrumentation.

## 154 REFERENCES

- 155 [1] J. Hak, Z. Johan, M. Kvacek, W. Liebscher, Kemmlitzite, a new mineral of the  
156 woodhouseite group, Neues Jahrbuch fuer Mineralogie, Monatshefte, 201-212,(1969)
- 157 [2] S.A. Makhmudov, C.M. Kashkai, Unit cell parameters of the alunite-group minerals and  
158 their structural analogs, Trudy Azerbaidzhanskogo Otdeleniya Vsesoyuznogo  
159 Mineralogicheskogo Obshchestva, 68-72,(1981)
- 160 [3] F. Novak, J. Jansa, Minerals of the crandallite and kemmlitzite group from Upper  
161 Carboniferous sediments at Bela and Libstat in the Krkonose piedmont basin, northern  
162 Bohemia, Vestnik Ceskeho Geologickeho Ustavu,72, 367-372,(1997)
- 163 [4] F. Novak, P. Paulis, J. Jansa, Crandallite, gorceixite, goyazite and kemmlitzite from  
164 pyrope-gravels of the Ceske stredohori Mts, Vestnik Ceskeho Geologickeho Ustavu,73, 107-  
165 111,(1998)
- 166 [5] F. Novak, P. Paulis, B. Moravec, Minerals of goyazite-svanbergite series and kemmlitzite  
167 from pyrope deposit Vestrev near Hostinne, northern Bohemia, Vestnik Ceskeho  
168 Geologickeho Ustavu,72, 373-380,(1997)
- 169 [6] R.L. Frost, E.C. Keeffe, S. Bahfenne, A Raman spectroscopic study of the antimonite  
170 mineral peretaite  $\text{Ca}(\text{SbO})_4(\text{OH})_2(\text{SO}_4)2\hat{\text{A}}\cdot 2\text{H}_2\text{O}$ , Spectrochim. Acta, Part A,75, 1476-  
171 1479,(2010)
- 172 [7] R.L. Frost, B.J. Reddy, E.C. Keeffe, Spectroscopy of selected copper group minerals:  
173 Chalcophyllite and chenevixite-implications for hydrogen bonding, Spectrochim. Acta, Part  
174 A,77, 388-396,(2010)
- 175 [8] R.L. Frost, Raman and infrared spectroscopy of arsenates of the roselite and fairfieldite  
176 mineral subgroups, Spectrochimica Acta, Part A: Molecular and Biomolecular  
177 Spectroscopy,71A, 1788-1794,(2009)
- 178 [9] R.L. Frost, Tlapallite  $\text{H}_6(\text{Ca,Pb})_2(\text{Cu,Zn})_3\text{SO}_4(\text{TeO}_3)_4\text{TeO}_6$ , a multi-anion mineral: A  
179 Raman spectroscopic study, Spectrochimica Acta, Part A: Molecular and Biomolecular  
180 Spectroscopy,72, 903-906,(2009)
- 181 [10] R.L. Frost, S. Bahfenne, J. Graham, Infrared and infrared emission spectroscopic study  
182 of selected magnesium carbonate minerals containing ferric iron-Implications for the  
183 geosequestration of greenhouse gases, Spectrochimica Acta, Part A: Molecular and  
184 Biomolecular Spectroscopy,71A, 1610-1616,(2009)
- 185 [11] R.L. Frost, J. Cejka, Near- and mid-infrared spectroscopy of the uranyl selenite mineral  
186 haynesite  $(\text{UO}_2)_3(\text{SeO}_3)_2(\text{OH})_2\hat{\text{A}}\cdot 5\text{H}_2\text{O}$ , Spectrochimica Acta, Part A: Molecular and  
187 Biomolecular Spectroscopy,71A, 1959-1963,(2009)
- 188 [12] R.L. Frost, J. Cejka, M.J. Dickfos, Raman spectroscopic study of the uranyl minerals  
189 vanmeersscheite  $\text{U}(\text{OH})_4[(\text{UO}_2)_3(\text{PO}_4)_2(\text{OH})_2]\hat{\text{A}}\cdot 4\text{H}_2\text{O}$  and arsenouranylite  
190  $\text{Ca}(\text{UO}_2)[(\text{UO}_2)_3(\text{AsO}_4)_2(\text{OH})_2]\hat{\text{A}}\cdot (\text{OH})_2\hat{\text{A}}\cdot 6\text{H}_2\text{O}$ , Spectrochimica Acta, Part A: Molecular  
191 and Biomolecular Spectroscopy,71A, 1799-1803,(2009)
- 192 [13] R.L. Frost, B.J. Reddy, S. Bahfenne, J. Graham, Mid-infrared and near-infrared  
193 spectroscopic study of selected magnesium carbonate minerals containing ferric iron-  
194 Implications for the geosequestration of greenhouse gases, Spectrochimica Acta, Part A:  
195 Molecular and Biomolecular Spectroscopy,72, 597-604,(2009)
- 196 [14] J.W. Anthony, R.A. Bideaux, K.W. Bladh, M.C. Nichols, Handbook of Mineralogy  
197 Vol.IV. Arsenates, phosphates, vanadates - Mineral Data Publishing, Tucson, Arizona,  
198 Mineral data Publishing, Tucson, Arizona, 2000.
- 199 [15] J. Emsley, Very strong hydrogen bonding., Chemical Society Reviews,9, 91-124,(1980)
- 200 [16] H. Lutz, Hydroxide ions in condensed materials - correlation of spectroscopic and  
201 structural data., Structure and Bonding (Berlin, Germany),82, 85-103,(1995)

202 [17] W. Mikenda, Stretching frequency versus bond distance correlation of O-D(H)...Y (Y =  
203 N, O, S, Se, Cl, Br, I) hydrogen bonds in solid hydrates., Journal of Molecular Structure,147,  
204 1-15,(1986)  
205 [18] A. Novak, Hydrogen bonding in solids. Correlation of spectroscopic and  
206 crystallographic data., Structure and Bonding (Berlin),18, 177-216,(1974)  
207 [19] E. Libowitsky, Correlation of the O-H stretching frequencies and the O-H...H hydrogen  
208 bond lengths in minerals, Monatshefte für chemie,130, 1047-1049,(1999)  
209  
210

211



212 *List of Figures*

213 **Figure 1a Raman spectrum of kemmlitzite in the 550 to 1200 cm<sup>-1</sup> region**

214 **Figure 1b Raman spectrum of kemmlitzite in the 500 to 900 cm<sup>-1</sup> region**

215 **Figure 2 Infrared spectrum of kemmlitzite in the 500 to 1800 cm<sup>-1</sup> region**

216 **Figure 3 Raman spectrum of kemmlitzite in the 100to 600 cm<sup>-1</sup> region**

217 **Figure 4 Raman spectrum of kemmlitzite in the 1000 to 1800 cm<sup>-1</sup> region**

218 **Figure 5a Raman spectrum of kemmlitzite in the 3000 to 3800 cm<sup>-1</sup> region**

219 **Figure 5b Infrared spectrum of kemmlitzite in the 2700 to 3100 cm<sup>-1</sup> region**

220

221

222

223

224

225

226

227

228

229

230

231

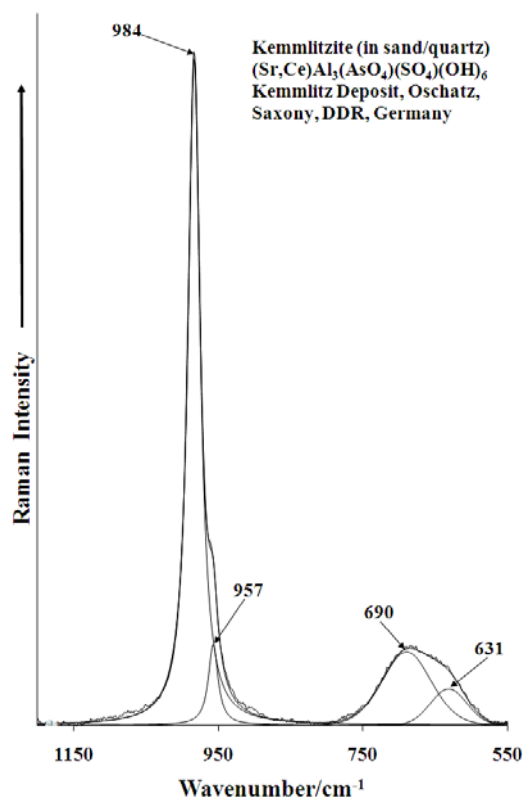


Figure 1a

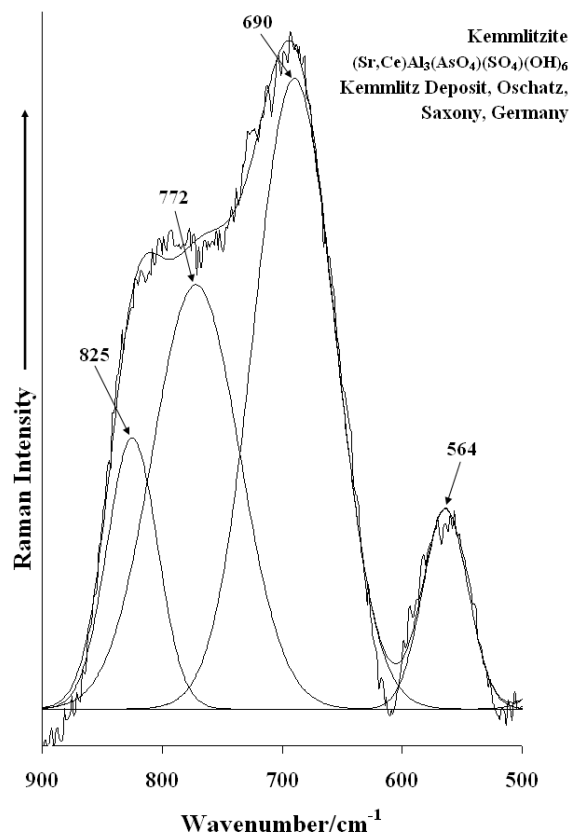
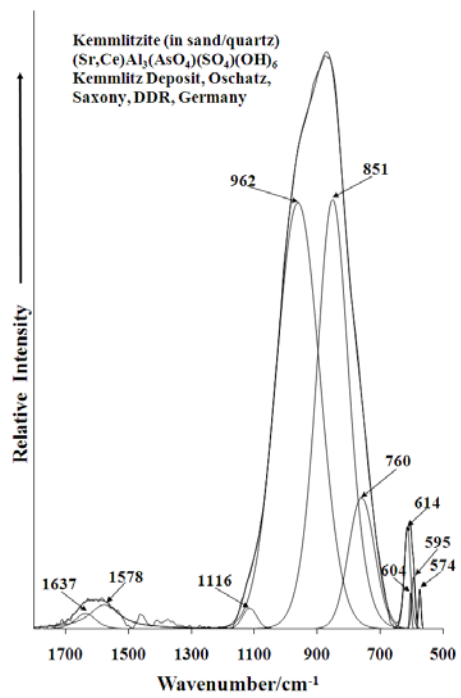


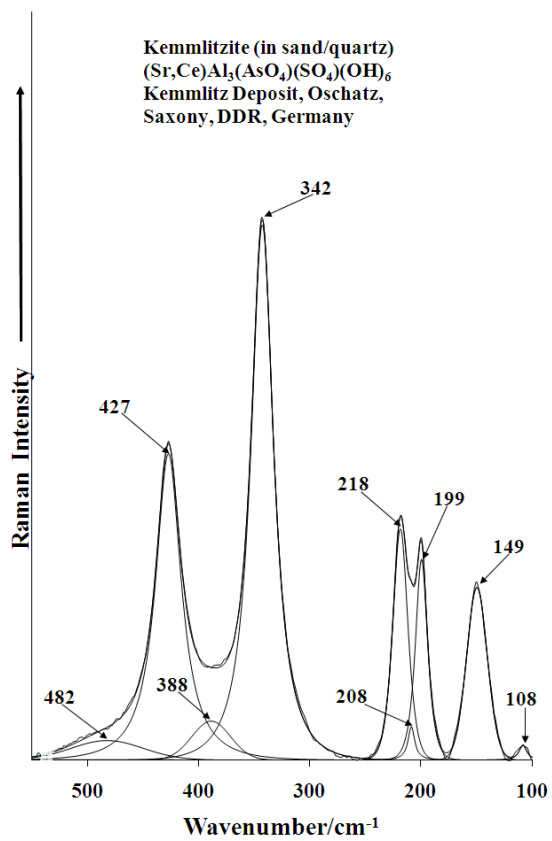
Figure 1b



236

237

238 **Figure 2**

**Figure 3**

240

241

242

243

244

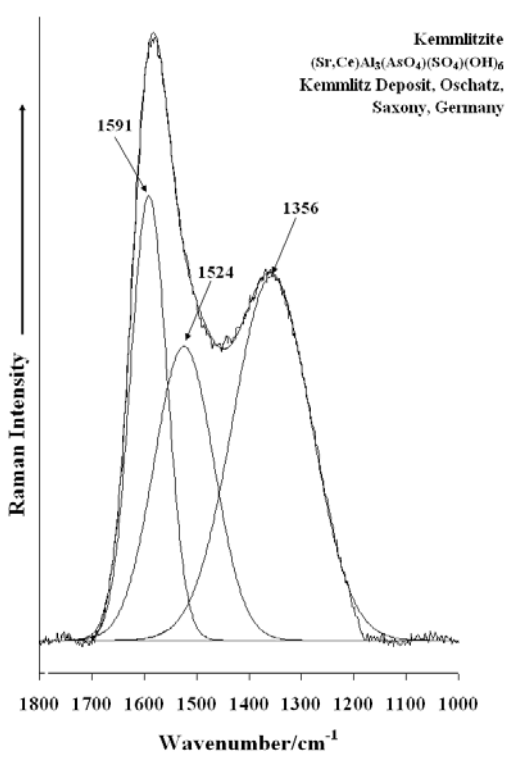
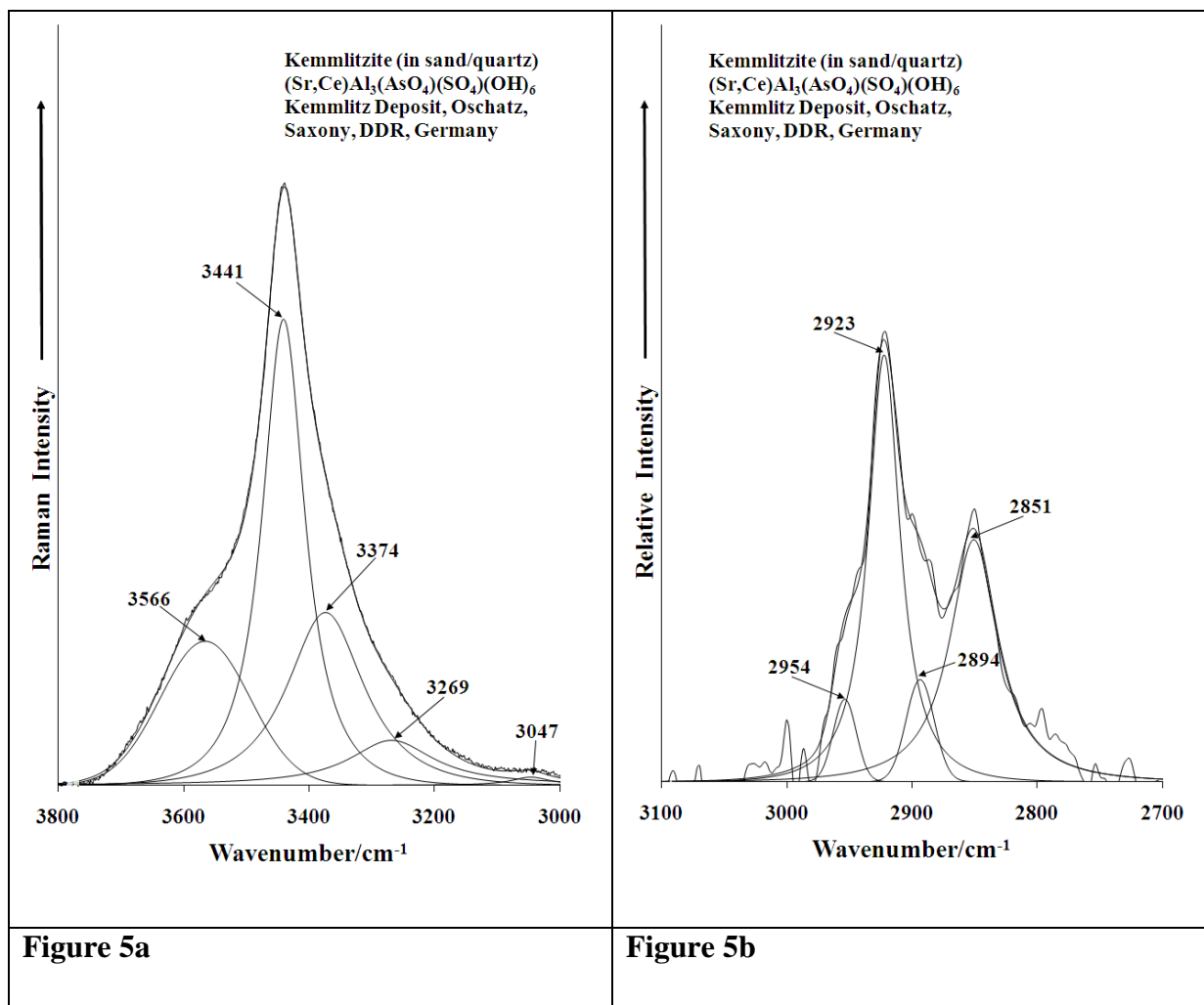


**Figure 4**

245

246

247



249

250

251